



Research Article

Influence of basalt fiber in ultra-high-performance concrete in hybrid mode: a comprehensive study on mechanical properties and microstructure

P Sujitha Magdalene¹ , B Karthikeyan² 

¹ Senior Research Fellow, School of Civil Engineering, SASTRA Deemed to be University, Tamilnadu (India), sujitha@civilsastra.ac.in

² Assistant Professor, School of Civil Engineering, SASTRA Deemed to be University, Tamilnadu (India), karthikeyan@civil.sastra.edu

Corresponding author: *karthikeyan@civil.sastra.edu

Received: 30.08.2023; **Accepted:** 03.02.2024; **Published:** 25.04.2024

Citation: Magdalene, P., Karthikeyan, B. (2024). Influence of basalt fiber in ultra-high-performance concrete in hybrid mode: a comprehensive study on mechanical properties and microstructure. *Revista de la Construcción. Journal of Construction*, 23(1), 104-128. <https://doi.org/10.7764/RDLC.23.1.104>

Abstract: The end, in view of the research, is to effectively utilize natural fiber (basalt) to reinstate the mechanical strength lost by the ultra-high-performance concrete (UHPC) matrix when the metallic steel fibers are quantitatively curtailed. Also, the river sand is fractionally ousted from the mixture, and manufactured sand is substituted. In addition to the preliminary constituents of UHPC, nano silica was adopted for the adequate packing of the matrix, which aids in strength-gaining reaction as well. To induce sustainability and implement waste utilization, two different proportions using M-Sand were made with 30% and 4% replacement levels, and for each proportion of M-Sand, five different mixes were made for varying fiber incorporation. Including the control mix made without any fiber, a total of 12 mixes were made. Among the fibrous mixes, two were metallic fibrous mixtures, and the rest were hybrid fibrous mixtures, and inter-comparisons were done accordingly. The metallic fibers were added in 1% and 2%, and natural fibers were incorporated in 1%, 2%, and 3% in volumetric fractions. From the trial mixes it was identified that the inclusion of Basalt fibers of more than 3% resulted in reduced workability, and so the addition of basalt fibers was restricted to 3%. The water-to-binder ratio of the UHPC matrix ranged between 0.15 and 0.17, depending upon the dosage of fibers. High range water reducer (HRWR) was mixed with water during casting, to develop the workability. The specimens were tested for compressive strength, split tensile strength, and impact energy resistance. It was identified that the annexation of 1% steel and 3% basalt fibers with 30% M-Sand was effective as they showed better compressive strength and impact resistance than the other combinations. Further Scanning Electron Microscopic (SEM) imaging and Thermogravimetric Analysis (TGA), which were conducted, also validated the inference from the experimental investigations.

Keywords: ultra-high-performance concrete, basalt fibers, impact energy resistance, post-cracking impact energy, ductility index.

1. Introduction

1.1 General

Ultra-high-performance concrete (UHPC) is now becoming the topmost debate in research and the construction industry (Voit & Kirnbauer, 2014). But, sustainability in construction is still a craving for the scientific community. In view of this, innovations in both materials and methods are the commitments to boost the lifespan of the structures (Ghafari et al., 2015). It is almost impossible for sulfates, chlorides, and CO₂ to enter the UHPC matrix, making it durable and dwindling maintenance (D. Wang et al., 2015). Both the microstructure and the lifespan of the early-age concrete were poor. Hence, as the primary reactive component, the part of cement in UHPC has to be at least three times higher than what is used in conventional or high-performance concrete. Sharma et al. (2022) suggested utilizing certain mineral admixtures like metakaolin, fly ash, and silica fume to assist in overcoming those limitations. But mineral admixtures are finite resources; moreover, mining them is a highly energy-consuming process. Karalar (2020) performed experimental and numerical investigations on RCC beams with bottom and fly ash. They also reflect adverse health effects, and hence the sprouting interest of researchers commenced focusing on alternate materials to cement (Wang et al., 2021). A few substitutes for cement, including rice husk ash, fly ash, silica fume, slag, or powdered glass, barely leave carbon traces, are economical, and enhance sustainable properties, recommended Du et al. (2021). Substituting lime powder, ground granulated blast-furnace slag (GGBFS), and fly ash for cement displays identical hydration behavior in the beginning, but GGBFS hastens the hydration as the days ascend (Yu et al., 2015). Van Tuan et al. (2011) developed UHPC with rice husk ash and confirmed that it is more effective than micro silica, but still, the micro silica combined with powdered glass delivered better strength (221 MPa) and the best pore size distribution. The silica fume not only fills the pores effectively but also lifts the hydration, which will be evident as the days go by (Abbas et al., 2016; Zhou et al., 2020).

Bajaber and Hakeem (2021) also later acknowledged that the silica fume has impressive mechanical and durable properties compared to GGBFS and fly ash. Though grey micro silica is more silicious, reactive, and has high carbon contents, white micro silica with zirconium can be utilized as it allows flowability and leaves carbon footprints to a smaller extent (Abdul-kareem et al., 2018). J. Zhang et al. (2017) experimented with the UHPC matrix by altering cement with fly ash and silica fume. They concluded that instead of 30% fly ash, only 10- 20% silica fume was effective, the author also noticed that a further increase in silica fume content gradually surged the compressive strength. Silica fume, being micro-sized, fills the micro pores, but the nanovoids also have to be considered for a denser matrix. Studies by Janković et al. (2016) and Wu et al. (2018) advised the utilization of nano-silica in UHPC, which helps in porosity reduction and the betterment of fiber-matrix bonds, microstructure, and mechanical strength and reported that compression and flexure resistances were elevated when 2% of nano-silica, where extra inclusion resulted in a decrease in strength. Aggregates are key to limiting the cost and shrinkage of concrete. The fine aggregates in UHPC are mostly river sand.

Though suggestive, it is a way of depleting the natural resource. So, to incorporate sustainability, many works are being done in the field of concrete to replace the river sand partially with industrial wastes. Memduh Karalar has done several works in incorporating different wastes in concrete, such as plastic waste (Korkut & Karalar, 2023), waste tyre (Karalar et al., 2023) and ceramic waste (Aksoylu et al., 2023). Research has been conducted on copper slag and iron ore tailings to replace river sand (Magdalene et al., 2023). There are traces of using aeolian sand or pre-wetted calcined zeolite sand (Chu et al., 2020; G.-Z. et al., 2020), but still, manufactured sand was found to be more effective in the UHPC matrix where 50% of it in place of natural (river) sand will not disturb the pore size distribution and hydration. (Yang et al., 2020) included manufactured sand in their UHPC research and inferred that it is more compact than river sand.

The concrete is designed for compressive strength every time, but the tensile strength and modulus of elasticity can still be upgraded only through fiber reinforcement. There are possibilities of reduced workability and raised porosity to abate the performance of UHPC (Yang et al., 2022). To reduce the brittleness in such concrete containing a large cement quantity, no coarse aggregate incorporation of fibers is preferred (Hou et al., 2018). However, the majority of the research works in UHPC focuses on using steel fibers and polymer fibers (Liu et al., 2022). The fibers are experts in improving tensile strength, but it has economic limitations. De Klerk et al. (2020) mentioned that synthetic and other manmade fibers are expensive and are also harmful due to the gases emitted during the manufacturing process. Park et al. (2012), in their research, mentioned that even a single percentage of fiber was more expensive than other materials. On the other hand, Yoo & Yoon (2015) disclosed that just 2% of steel fibers cropped up one-third of the cost of their whole UHPC mixture. Dingqiang et al. (2021) also

recommend restricting the fibers to 2% to establish dense packing. Steel fibers are frequently used; nevertheless, it has economical and corrosion constraints. Also, it hikes the dead load of the structure as they are denser. They possess aesthetic drawbacks as well, in terms of surface finish. Du et al. (2021) quote the works accomplished with other synthetic and natural fibers to encounter the limitations of steel fiber. Basalt fibers also play a vital role as an alternative to steel fibers, and research works state that basalt fibers, when included in the UHPC matrix, could postpone the formation of diagonal cracks (Jabbar et al., 2021). But the limitation is, the higher the fiber dosage, the less will be the workability. Yan et al. (2021) addressed that compression and flexure show favorable results when glass fibers are used. A percentage of polypropylene fiber would give higher compressive and split tensile strength results, but only 0.2% of basalt fibers can collectively improve every concrete property (Gao et al., 2021; Prasad et al., 2018).

The absence of fiber generates brittle failure, yet the fractions and length of the fibers should be considerable (Wiemer et al., 2020). Lowering the water-to-binder ratio leads to high-quality concrete, but no appreciable elevations were disclosed in the case of microfibers over 1.5% (Mohammed et al., 2021). There is evidence of employing asbestos fibers, but they are discontinued from application owing to their health risk (Bajaber & Hakeem, 2021). Ren et al. (2021) researched sisal fibers and reported that they have a minor impact on strength but provide sufficient ductility. Though many other fibers, such as polypropylene, glass, basalt, sisal, and several other fibers, were suggested as alternatives for steel fibers, there are a few drawbacks to using them individually. Onur Pehlivan (2022) mentioned that the incorporation of basalt fibers improved the flexural properties as well as the fracture energies. Aimin et al. (2024) reported that even though Sisal fibers provided better-reinforcing effects on UHPC, the cost of sisal fibers is higher than that of UHPC.

It is the same reason for which the research works using non-metallic fibers as mono fibers are scarcely available, and the use of hybrid fibers is encouraged as the different fibers can be chosen based on the size and shapes, which will yield less fiber content overall (Zeimei. et al., 2016). Kim et al. (2011) observed and reported that using short fibers could bridge the micro-cracks, and large fibers could reduce the propagation of major crack gaps. As stated in the literature discussed, it is evident that many researchers prefer UHPC with hybrid fibers. also, it can be noted that most of the works focus on using steel and polypropylene fiber. Khan et al. (2024) mentioned that the other advantage of using hybrid fibers, especially those with steel basalt, is reducing the spalling effect in ultra-high performance. In the current research, a hybrid UHPC composite has been made using steel fiber and basalt fiber. Different combinations of hybrid UHPC composites were made for different proportions of basalt fiber addition and for varying proportions of M-Sand. The influence of basalt fiber in resisting the impact loads was analyzed and reported.

1.2 Research significance

The utilization of non-metallic fibers is less in the research on UHPC so far. The current work is desired to develop a sustainable UHPC mix using waste materials without compromising the strength. In this regard, M-sand and basalt fiber were used as fine aggregates and fiber reinforcements in the UHPC mix. The research goes beyond the conventional use of river sand in UHPC and explores the potential benefits of incorporating manufactured sand, emphasizing its compactness compared to river sand. The study focuses on the environmental concerns associated with traditional materials and seeks alternatives that are mechanically effective and sustainable. The research emphasizes utilizing alternative non-metallic fibers such as basalt fiber for steel fiber and brings out the advantage of developing UHPC in hybrid mode.

2. Materials and methods

2.1. Materials

Cement, Silica fume, nano silica, river sand, Manufactured sand (M-sand or MS), metallic and non-metallic fibers, high-range water reducer, and potable water were chosen for the mix based on the previous research.

2.1.1. Cementitious materials

2.1.1.1. Cement

Conforming to ASTM C150 (2022)., Penna Premium ordinary Portland cement (OPC) 53-grade cement manufactured by Penna Cement Industries, Hyderabad, India, was utilized for the UHPC mix production. Initially, the cement was subjected to X-ray Fluorescence (XRF) to obtain its elemental composition, as shown in Table 1. As it is the traditional binder and primary reactive component, certain preliminary tests, including the specific gravity and setting times, were conducted. Cement mortar cubes were also tested for the 28-day compressive strength, conforming to IS-4031-PART-6 (1988) It was also made sure that the material had an optimum particle size distribution and crystallized structure.

2.1.1.2. Silica fume

Grey silica fume, with more than 99% silica content confirmed by XRF, was adopted for the research. It covered up around 8% of the whole cementitious content of the UHPC mixture. Figure 1 shows the silica fume utilized for the mix.

2.1.1.3. Nano silica

Nano silica in dust form comprised of almost only silica was used. The chemical composition that confirms the presence of silica is shown in Table 1, wherein all the other oxides are negligible. Since the material was highly lightweight, as shown in Fig 1, mixing it with water to make a gel before adding it to the mix was mandatory. As per the recommendations from the literature, 2% of nano silica occupied the cementitious content.

Table 1. XRF of the cementitious materials.

Oxide form (in %)	Formula	CaO	SiO ₂	Fe ₂ O ₃	Al ₂ O ₃	SO ₃	K ₂ O	MgO	TiO ₂	Na ₂ O
	OPC	65.13	19.15	5.86	3.83	3.62	0.80	0.77	0.25	0.19
	Silica fume	0.24	99.02	0.05	0.31	-	-	0.03	-	0.05
	Nano silica	0.03	99.81	73ppm	-	-	-	-	-	0.06



Figure 1. Cementitious materials.

2.1.2. Aggregates

2.1.2.1. River sand

The local river sand procured was sieved and the gradation curve was arrived as shown in Figure 2. Sand contents not more than 1.18mm were considered for the research to ensure better packing of the materials.

2.1.2.2. Manufactured sand

To effectively employ industry waste in the UHPC mix and prevent the exhaustion of natural deposits, manufactured sand has been included as a fractional alternative for river sand. Manufactured sand less than and equal to 600 microns in size was selected to end up with dense packing of the matrix. Two disparate proportions of 70:30 (MS1) and 60:40 (MS2) ratios of

river and manufactured sand were investigated separately and compared. Figure 3 displays the surface-saturated river and manufactured sand used in the investigation.

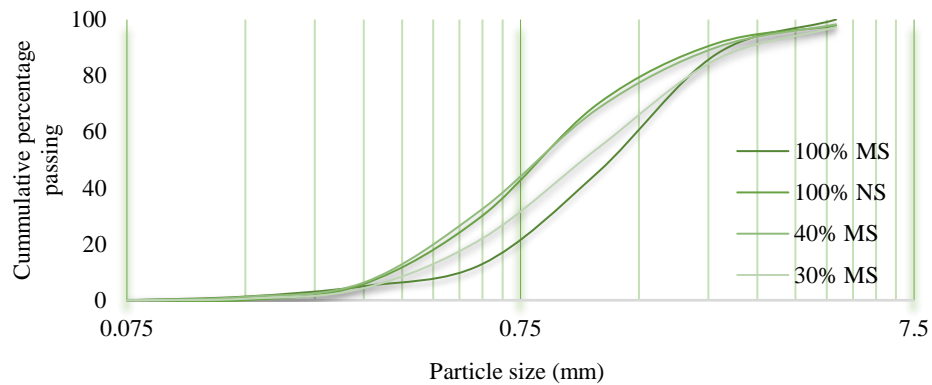


Figure 2. Aggregate gradation.



Figure 3. Fine aggregates.

2.1.3. Metallic and non-metallic fibers

2.1.3.1. Steel fiber (SF)

Figure 4 shows the microscopic detailing of steel fibers, where 12mm long crimped steel fibers with 0.5mm diameter were used. The aspect ratio of the fibers was determined to be 24. The density and tensile strength of the fibers were 7850 kg/m³ and 1176 MPa, as specified by the dealer.



Steel fibers



Length of fiber



Diameter of fiber

Figure 4. Details of steel fiber.

2.1.3.2. Basalt fiber (BF)

Chopped filaments of basalt fibers, as shown in microscopic images of Figure 5, with 6mm length and 1.5mm breadth, were used. a single filament containing numerous strands of fibers evenly dispersed during mixing. As per the data from the dealer, the density was 2650 kg/m³, and the tensile strength was 4470 MPa.

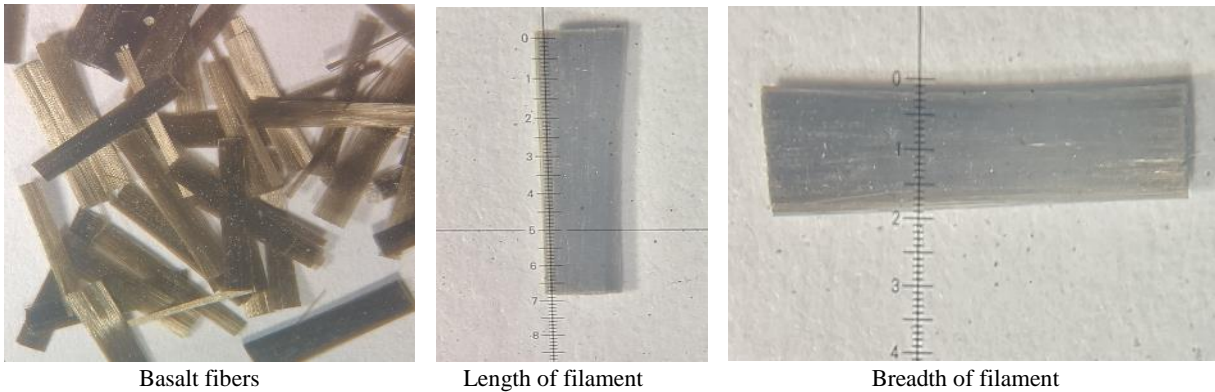


Figure 5. Details of basalt fiber.

2.1.4. Chemical admixture

Sika® Viscocrete® – 20 HE, a light brown aqueous solution based on polycarboxylates procured from the dealer, was used as the chemical admixture for the UHPC mix. The pH was greater than 6 with a density of 109 kg/l, which the dealer specified. The admixture was well dispersed in locally available potable water before use.

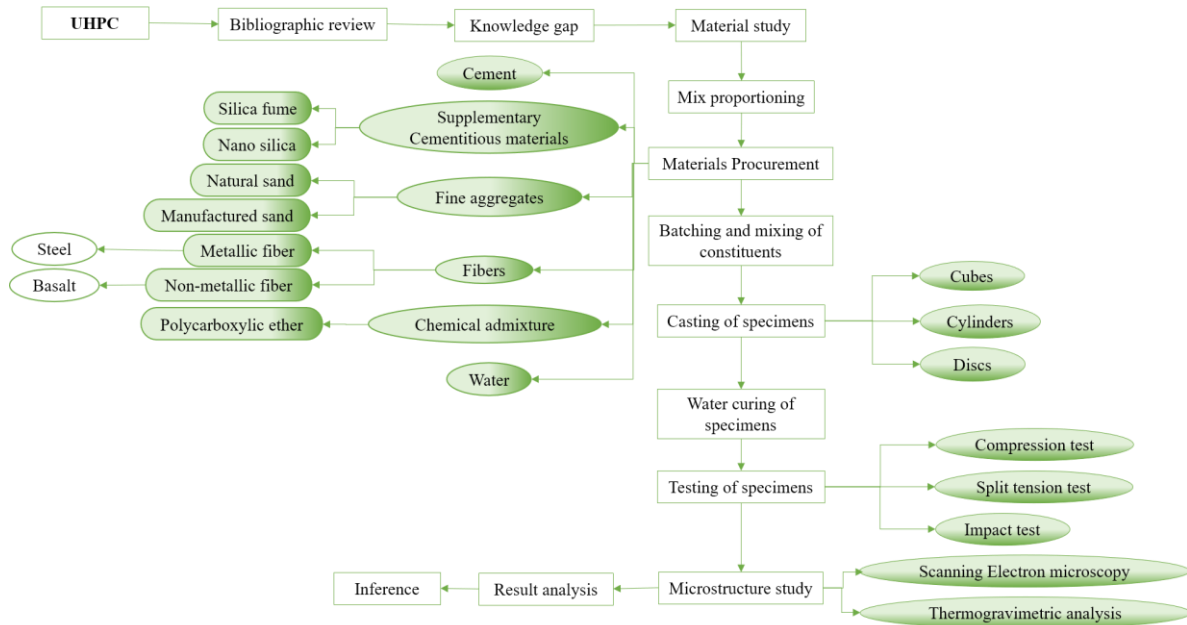


Figure 6. Flow of research.

3. Experimental investigations

3.1. Methodology, mix proportions, and mixing details

As detailed in the research flow, Figure 6, the materials were procured, and the specimens of cubes (70.7mm x 70.7mm x 70.7mm), cylinders (128mm height; 64mm diameter), and discs (160mm diameter; 65mm height) were cast. The method of weight batching was adopted as per the mix proportions specified in Table 2 and Table 3.

Table 2. Mix proportion of MS1.

Sl. no	Mix ID	Material constituents								
		Cement	Silica fume	Nano silica	River sand	M-sand	Water	HRWR	SF (%)	BF (%)
(in kg/m ³)										
1	NF						135	12.15	-	
2	F-S-1						139.5	12.33	1	-
3	F-S-2	810	72	18	700	300	144	12.555	2	-
4	F-SB-1						145.8	12.6	1	1
5	F-SB-2						148.5	12.87	1	2
6	F-SB-3						151.2	13.185	1	3

Table 3. Mix proportion of MS2

Sl. no	Mix ID	Material constituents								
		Cement	Silica fume	Nano silica	River sand	M-sand	Water	HRWR	SF (%)	BF (%)
(in kg/m ³)										
1	NF						135	12.15	-	
2	F-S-1						139.5	12.33	1	-
3	F-S-2	810	72	18	600	400	144	12.555	2	-
4	F-SB-1						145.8	12.6	1	1
5	F-SB-2						148.5	12.87	1	2
6	F-SB-3						151.2	13.185	1	3

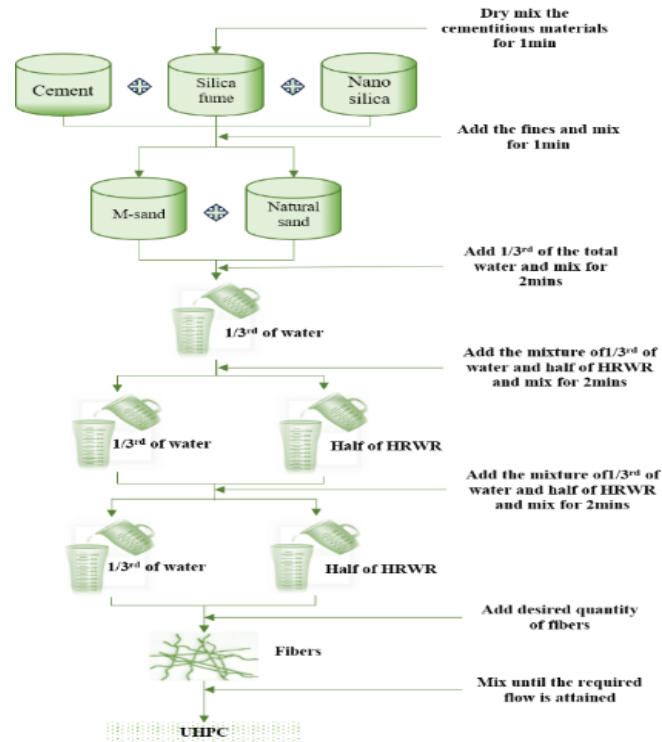


Figure 7. Mixing procedure.

Figure 7 elaborates on the typical mixing procedure maintained throughout the research, where the cementitious materials were blended in the drum mixer for about a minute, and the pre-wetted surface-saturated sand (both river and manufactured) was included in the mixer. Once the thorough dispersion is ensured the water and HRWR were poured in parts. The mix sounded dry in the beginning but the chemical admixture gave hands and developed the workability (Figure 8). The water-to-binder ratio and the dosage of HRWR for different types of fibers and their dosages are shown in Figure 9.



Figure 8. Mixing – intermediate stage and final mix.

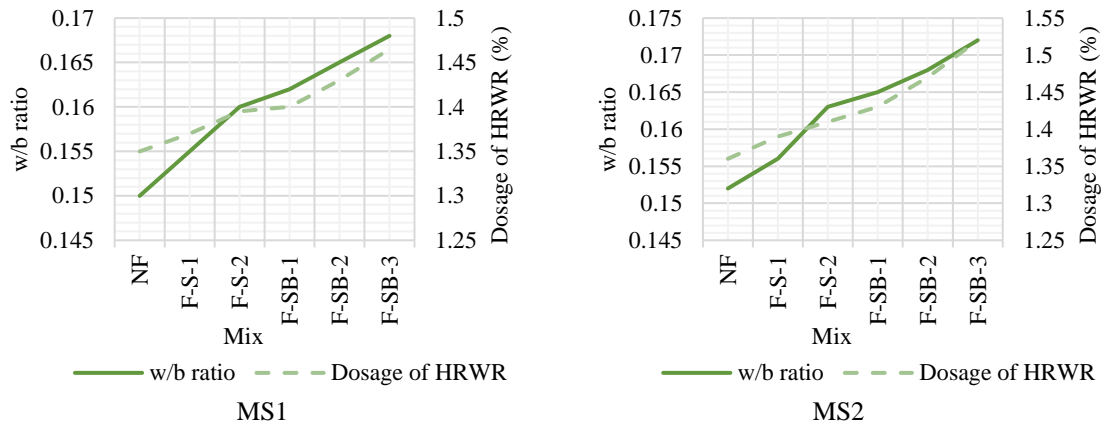


Figure 9. Variation in w/b ratio and HRWR dosages.

The desired fiber proportions were included in the mix after the flow was attained. It was desired to use 2% of steel fibers in volumetric fractions, in which the natural fibers substituted 1% of steel fibers. The hybrid fibrous UHPC mix had up to 3% natural fiber with good workability, and further inclusion of fiber ended up in the balling effect of concrete (Figure 10). Therefore, further addition of fibers was stopped.



Figure 10. Balling effect due to further addition of basalt fiber.

The fresh concrete mixture was tested for flow as specified in ASTM C1437 (2015) and is shown in Figure 11. The flow as the ASTM standard is calculated by Equation (1) as follows:

$$Flow (\%) = \frac{\text{Increment in diameter} - \text{original diameter} \text{ of mortar base}}{\text{Original diameter of mortar base}} \quad (1)$$

All the mixtures with and without fibers satisfied the flowability.



Figure 11. Workability investigation.

The mix was poured into the mould, and as per ASTM C1856 (2017), the tapping rod and vibrator were avoided, and the sides of the moulds were gently tapped. As suggested in ASTM C192 (2020), the specimens were covered with a sheet before

hardening immediately after finishing. It took 36 hours minimum for the specimens to harden due to the addition of admixture. The method of moist curing was adopted, where the specimens were immersed in water for the whole curing period as per the same ASTM standard. The specimens were ambient dried (Figure 13) once the curing (Figure 12) was over, and the desired tests were performed.



Figure 12. Specimens under curing.



Figure 13. Sample of specimens before testing.

3.2. Tests on hardened concrete

3.2.1. Test for compression

Specimens of dimensions 70.7mm x 70.7mm x 70.7mm, as mentioned in IS-4031-PART-6 (1988), were cast and using a hydraulic compression testing machine of capacity 3000 kN, the specimens were tested at a loading rate of 0.572 kN/sec as shown in Figure 14.



Figure 14. Compressive strength test.

3.2.2. Test for split tensile strength

Cylindrical specimens confirmed to the specification in, ASTM C470 (2023) were used, where the height of the specimen was twice the diameter. The test was performed with a hydraulic compression testing machine of 3000 kN load capacity. Figure 15 shows the splitting tensile strength test on UHPC cylinders. The splitting tensile strength of the specimens was calculated using Equation (2) as follows:

$$\sigma = \frac{2W}{\pi dl} \quad (2)$$

where W is the maximum tolerated by the specimen before splitting, and d and l are the diameter and length of the specimens, respectively.



Figure 15. Splitting tensile strength test.

3.2.3. Test for impact energy resistance

A drop weight impact testing machine shown in Fig 16ure was used to test the specimens for impact energy resistance. Specimens of dimensions confirming to ACI 544 – 2R– 89 (2002) were tested using an iron ball of 4.54 kg allowed to freely fall from 457mm height as per the guidelines of ASTM D1557 (2021). The number of blows required to crack the specimen initially and the number of blows to collapse the specimen completely were noted, and the impact energy resistance was determined in joules. Post-cracking energy resistance and ductility indices were also calculated using the initial and final number of blows.

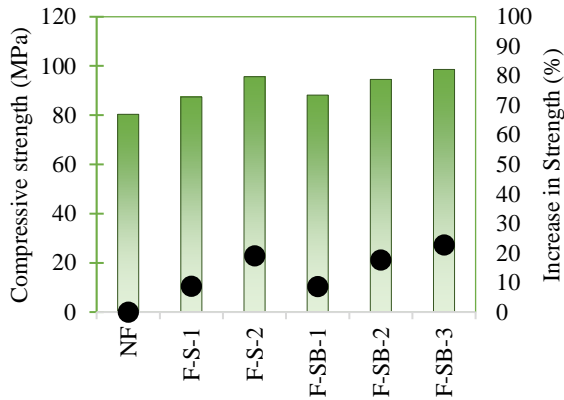
$$\text{Impact energy resistance} = W \times h \times n \quad (3)$$

where W is the iron ball weight, h is the height of fall from the top surface of the specimen, and n is the number of blows.

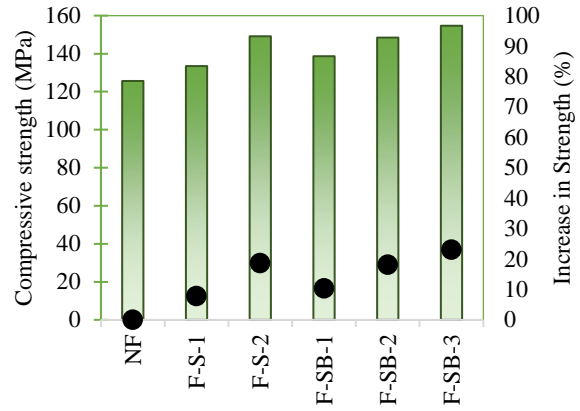


Figure 16. Test for impact energy resistance.

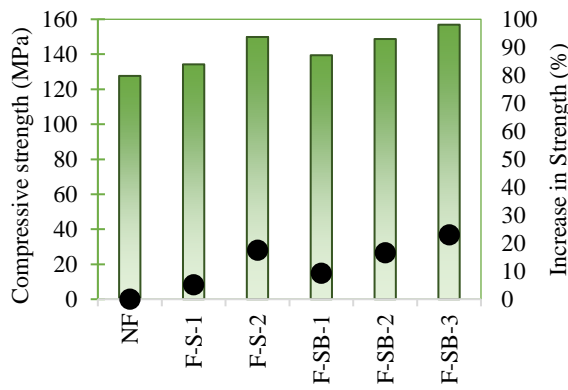
4. Results and discussion



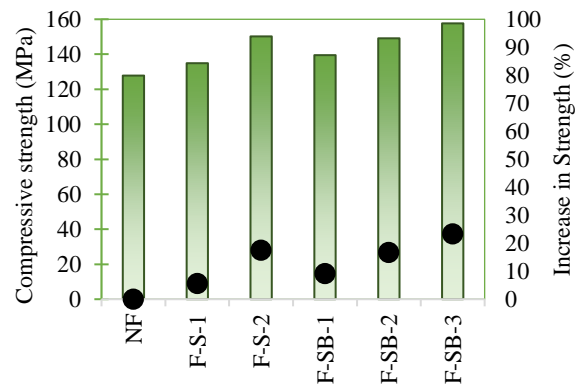
Concrete mix ID
(a) MS1 – 7 days curing



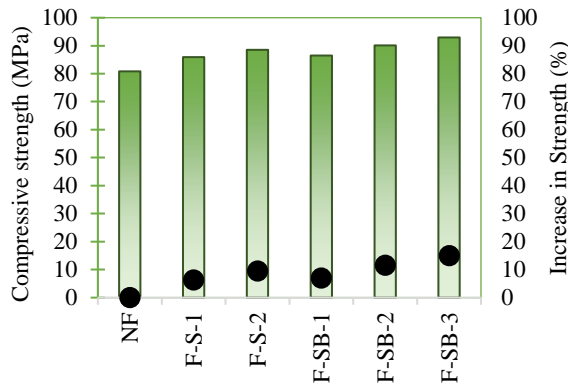
Concrete mix ID
(b) MS1 – 28 days curing



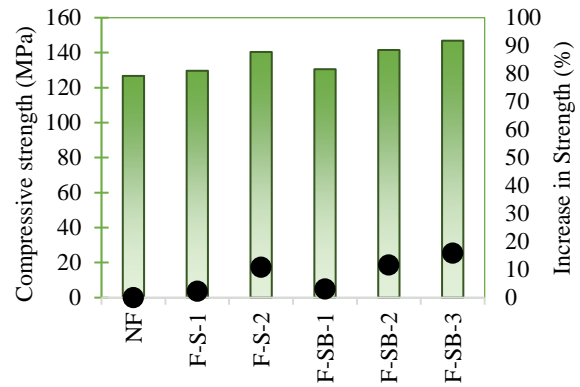
Concrete mix ID
(c) MS1 – 56 days curing



Concrete mix ID
(d) MS1 – 90 days curing



Concrete mix ID
(e) MS2 – 7 days curing



Concrete mix ID
(f) MS2 – 28 days curing

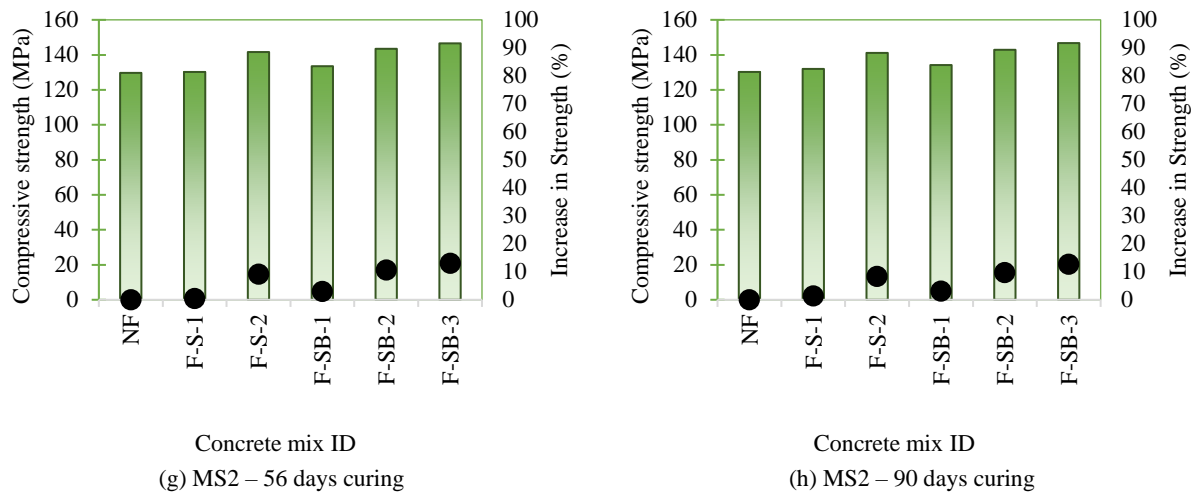


Figure 17. Compressive strength results.

4.1. Analysis of resistance to compression

Figures 17 (a) to 17 (g) illustrate the behavior of specimens cast with MS1 and MS2-type fine aggregates for different fiber proportions. The results are presented for different curing ages, namely early age curing, like 7 days, normal 28 days curing, and long-term curing, such as 56 and 90 days, to examine the rate of increase in strength when exposed to curing for longer durations. The first bar of every chart represents the strength development of the NF mix. The absence of fibers in UHPC was highly favorable in workability. The flow nearly resembled that of self-compacting concrete, and the mix was easy to handle and fill. MS1 showed better flow properties than MS2, possibly due to higher moisture in river sand than in manufactured sand as it is an industrial waste. The compressive strength plot shows that all the mixes have attained the minimum required compressive strength for UHPC, which is 120 MPa, as per ASTM C1856 (2017). Though the same standard suggests that UHPC mixtures are generally made with fibers, a non-fibrous (NF) mix was made to compare it with the metallic and hybrid fibers. The failure was brittle in the case of compression, where the structure’s integrity was absolutely lost. As with the other types of concretes, strength development was tremendous at the initial ages of curing, but the mixture led to a nearly constant strength between 56 and 90 days of curing. Roughly 60 to 65% of the concluding strength of the mixture at 90 days was developed at 7 days of curing. Only 1-2% of the strength was developed from 28-90 days in both the cases MS1 and MS2.

Incorporating basalt to alter 1% steel was highly effective, and the curve trend has grown throughout. Referring to Figure 17 (a) to (h), it is evident that the F-SB-1 could not balance the strength of F-S-2 but worked better than F-S-1 in both fine aggregate cases. For the mixes with MS1 in which M-Sand was replaced for river sand in 30%, larger compressive strength was possessed by FS2 in metallic fiber combination for an incorporation of 2% steel fiber. A maximum strength of 95.64 MPa in 7 days and a drastic increase to about 149.14 MPa in 28 days was observed. After 28 days, the strength increased; though it existed, it was at a slower rate only. At 56 days and 90 days, the FS2 specimen exhibited 149.88 MPa and 150.22 MPa, which were only 0.497% and 0.724% increases in compressive strength at 28 days. Whereas a 55.94% strength increase was noted for the specimen in 28 days from 7 days. It was analogous to the studies by Huang et al. (2023) that F-S-1 mix with MS1 & MS2 gained an average of 6.8% and 2.59%, and F-S-2 mix with MS1 & MS2 gained an average of 18.2% and 9.46% compressive strength more than NF respectively. The randomly dispersed fiber in various angles benefitted in obstructing the cracks developed while loading, and the specimen structure did not entirely collapse, as discussed by Yang. et al., (2023). Another notable count was that the corrugations in the steel fibers inhibited the slippage between concrete and fiber. Figure 17 (a) to (h) shows the comparative plot between the compressive strengths of various fiber dosages. The NF mix, during testing, exhibits an explosive failure form, which was suppressed with the addition of steel fibers. As reviewed by Rui et al. (2022), the observable formation of a skeletal grid of steel fiber supported the matrix to escalate the strength with a raised fiber quantity.

Among the hybrid fiber combinations, FSB3 possessed the highest strength of 98.59 MPa and 154.68 MPa in 7 days and 28 days, respectively. Exposing them to a curing period of 56 and 90 days resulted in a 1.441% and 1.93% increase, respectively.

Specimens with MS2 as fine aggregate possessed higher strength for FSB3 combination in 7, 28, 56, and 90 days of normal curing. As in the earlier case, i.e., in MS1, the specimens with metallic fiber incorporated showed strength attainment of 88.52 and 140.41 MPa in 7 and 28 days, and the rate of strength increase in 56 days and 90 days was found to be less. The hybrid fiber combination in specimens showed a gradual strength increase when non-metallic fiber presence was increased from 1% to 3%. The maximum non-metallic fiber addition was restricted to 3% as the addition of fibers more than this range affected the workability of the mix.

The graph also presents the percentage increase in strength of each fiber dosage with respect to NF. F-SB-1 gained an average of 9.62% compressive strength more than NF with MS1, but the same was only 4% with MS2. Identical patterns of increase in compressive strengths were spotted for F-SB-2 and F-SB-3, where 17.25% with MS1 and 10.88% with MS2 for the former, 23.03% with MS1 and 14.14% with MS2 for the later. The strength complemented by basalt fibers agrees with the studies by Harish et al. (2023), which may be because of the better dispersion of basalt than steel fibers. Basalt fibers also promote the dimensional stability offered by the coarse aggregates in other concrete types.

4.1.1. Overall comparison

Among the mix categories cast for compressive strength, those that were cured for 28 days of normal curing were considered for comparison. The FSB3 specimen made with MS1 fine aggregate, 1% steel fiber, and 3% basalt fiber registered the highest compressive strength of 154.64 MPa. The same fiber incorporation for MS2 fine aggregate has shown a compressive strength of 146.86 MPa with a strength decrease of 5.03%. One of the reasons for the decrease in strength of the specimens cast using the MS2 category may be the presence of more M-Sand, as they were used as a replacement for river sand in 40%. There may not be proper interlocking between the aggregates. As it is an industrial waste, it will be available in different sizes; even though care was taken to utilize the particles with sizes equal to or less than that of river sand, they lack the proper shape that the river sand possesses. Sujitha Magdalene et al. (2023) reported that the performance of the UHPC specimens made with Iron ore tailings and industrial waste as a replacement for river sand, 40%, was less than that of the UHC made with 30% IOT as a replacement and reported that the reason might be due to the lack of the interlocking and packing capabilities of the river sand, another reason may be due to the incorporation of more non-metallic fibers. In the present research, it was felt that adding Basalt fiber affected the workability, so it was restricted to 3%. These observations confirm the views of Yoo et al. (2017), Qi et al. (2018), and Zhang et al. (2019) on using deformed fibers in UHPC that the non-metallic fibers are vulnerable to agglomeration in the mixes and affect the flowability severely. Even then, less workability was managed with the suitable addition of superplasticizers. Non-metallic fibers create a balling effect that affects the workability of the mix and affects the bonding of the aggregates, thereby affecting the strength. The less workability due to the incorporation of more fibers and also the use of more M-Sand, on the whole, affected the strength characteristics of the MS2 mix.

4.2. Analysis of resistance of split tensile strength

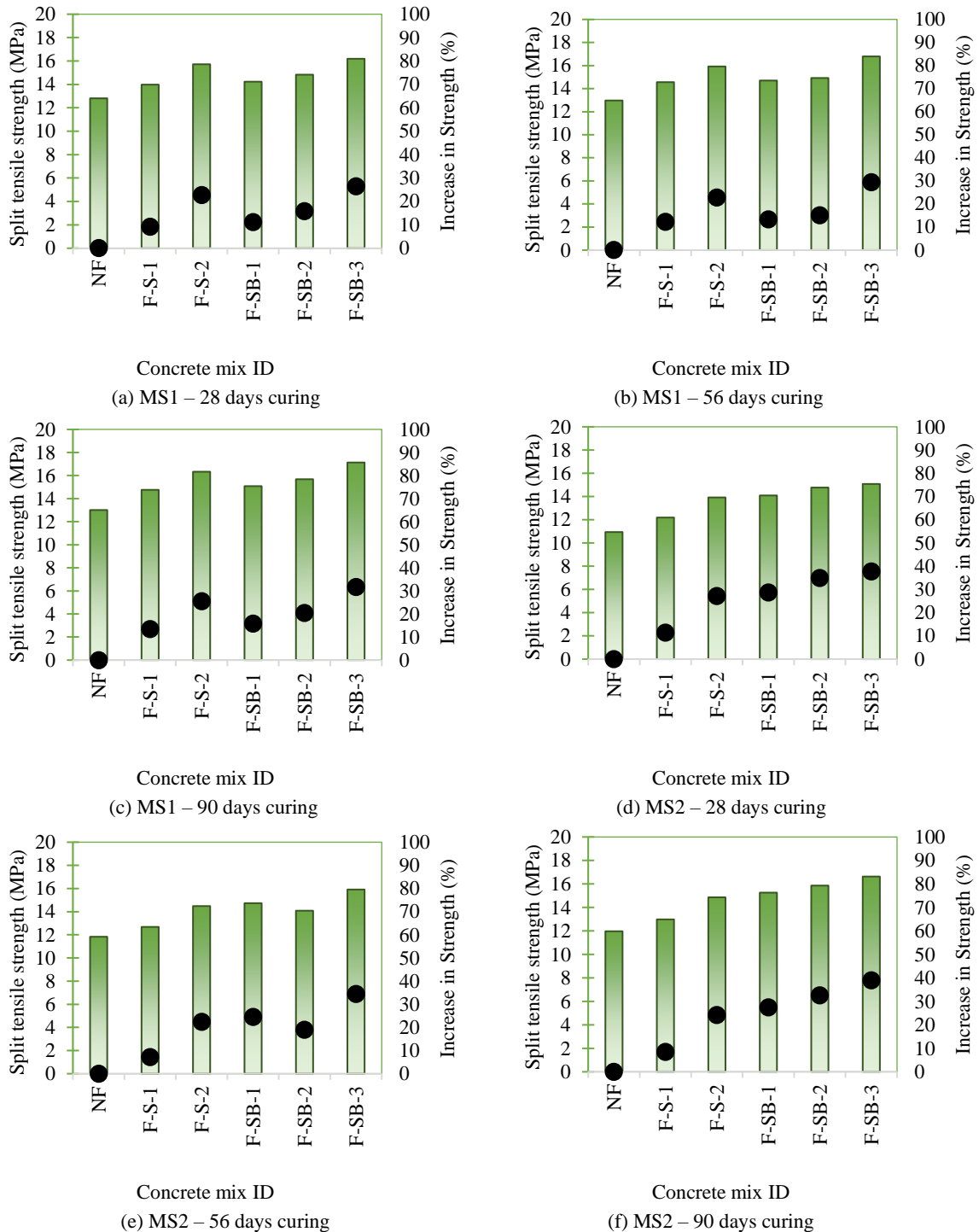


Figure 18. Splitting tensile strength results.

The splitting tensile strength results for 28 days, 56 days, and 90 days are illustrated in Figure 18 (a) to 18 (f). On satisfying the compression parameter, NF was subjected to the tensile test where the outcomes were satisfactory that the values fell between 1/10-1/8 of the compressive strength, but sudden unexpected collapse was noticed. On comparing the tensile strength

resisting capability of F-S-1 and F-S-2 specimens made with 1% and 2% steel fiber and for MS1 and MS2 aggregates and comparing them with specimens with control mix, which was made with no fiber incorporation (NF), it is observed that those made using MS1 category showed higher resistance to split than the NF mix. The split tensile strength of F-S-1 and F-S-2 with MS1 recorded an average increment of 11.61% and 23.66%, respectively. The steel fiber enhanced the crack-bridging mechanism, and the specimen remained intact even post-failure.

The same trend observed in compressive strength was seen in the tensile strength behaviour also. Here too, the incorporation of more fibers with moderate replacement of M-Sand improved the tensile strength.

Among the metallic fibers, F-S-B-3 with 3% basalt fiber incorporated exhibited the highest tensile strength of 16.79 and 15.08 MPa for the MS1 and MS2 categories in 28 days. Though there was a strength increase in 56 and 90 days, the rate of increase was less.

With MS2, the splitting tension of both the mixes was 9.02% and 24.59% higher than NF. FSB3 with 3% basalt fiber and with MS2 fine aggregate showed less strength. As mentioned earlier, MS2 has more partial replacement of river sand by M-Sand. The improper interlocking among the aggregates might have developed larger gaps between the aggregates. Though the fibers could bridge them, it was effective when the replacement level was used in a nominal replacement level of fine aggregates like the one used in the MS1 category.

4.2.1. Overall comparison

The split tensile strength of basalt fiber-reinforced UHPC functioned well so that no detachments were seen on the specimens. The resistance to split tension increased with increased fiber dosages at an average of 13.45% with MS1 and 26.93% with MS2 for F-SB-1, 17.11% with MS1 and 28.84% with MS2 for F-SB-2 and 29.17% with MS1 and 37.09% with MS2 for F-SB-3, respectively the split tension comparisons and increase in tensile strength, shown in Figure 18(a) to 18 (f) is relative to the review by Al-Rousan et al., (2023), where the authors assure a surge in split tensile strength with increasing basalt fibers. Basalt fibers could exhibit only average resistance to impact, and F-SB-3 could render a tolerance equivalent to F-S-2. F-SB-1, F-SB-2, and F-SB-3 were determined to have 61.94%, 49.59%, and 43.77% with MS1 and 67.83%, 58.16%, and 45.12% with MS2 higher ductility than NF, respectively.

4.3. Analysis of resistance to impact force

Table 4. Blows count in the impact test.

Aggregates	MS1						MS2					
	28 - days		56 - days		90 - days		28 - days		56 - days		90 - days	
Curing age	No. of blows											
Mixture ID	Initial crack	Final crack										
NF	161	582	182	602	204	621	173	608	197	627	215	638
F-S-1	193	1072	207	1093	219	1124	196	1093	210	1119	221	1147
F-S-2	231	1230	250	1278	261	1309	239	1239	252	1293	267	1337
F-SB-1	203	1161	223	1188	244	1236	208	1173	227	1204	242	1248
F-SB-2	239	1201	253	1272	274	1315	233	1208	251	1289	270	1324
F-SB-3	257	1252	271	1289	290	1348	261	1261	279	1297	296	1331

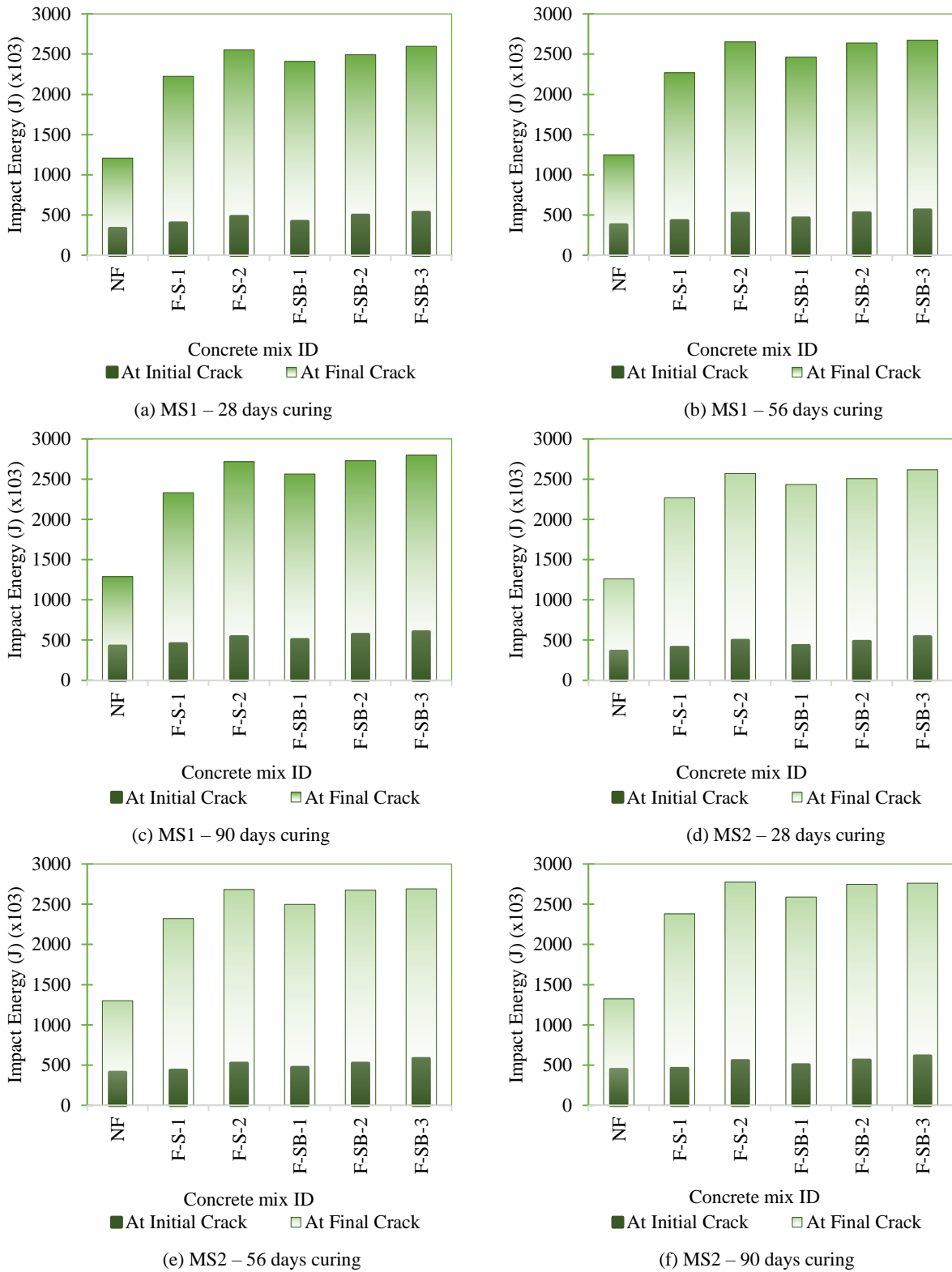


Figure 19. Impact energy results.

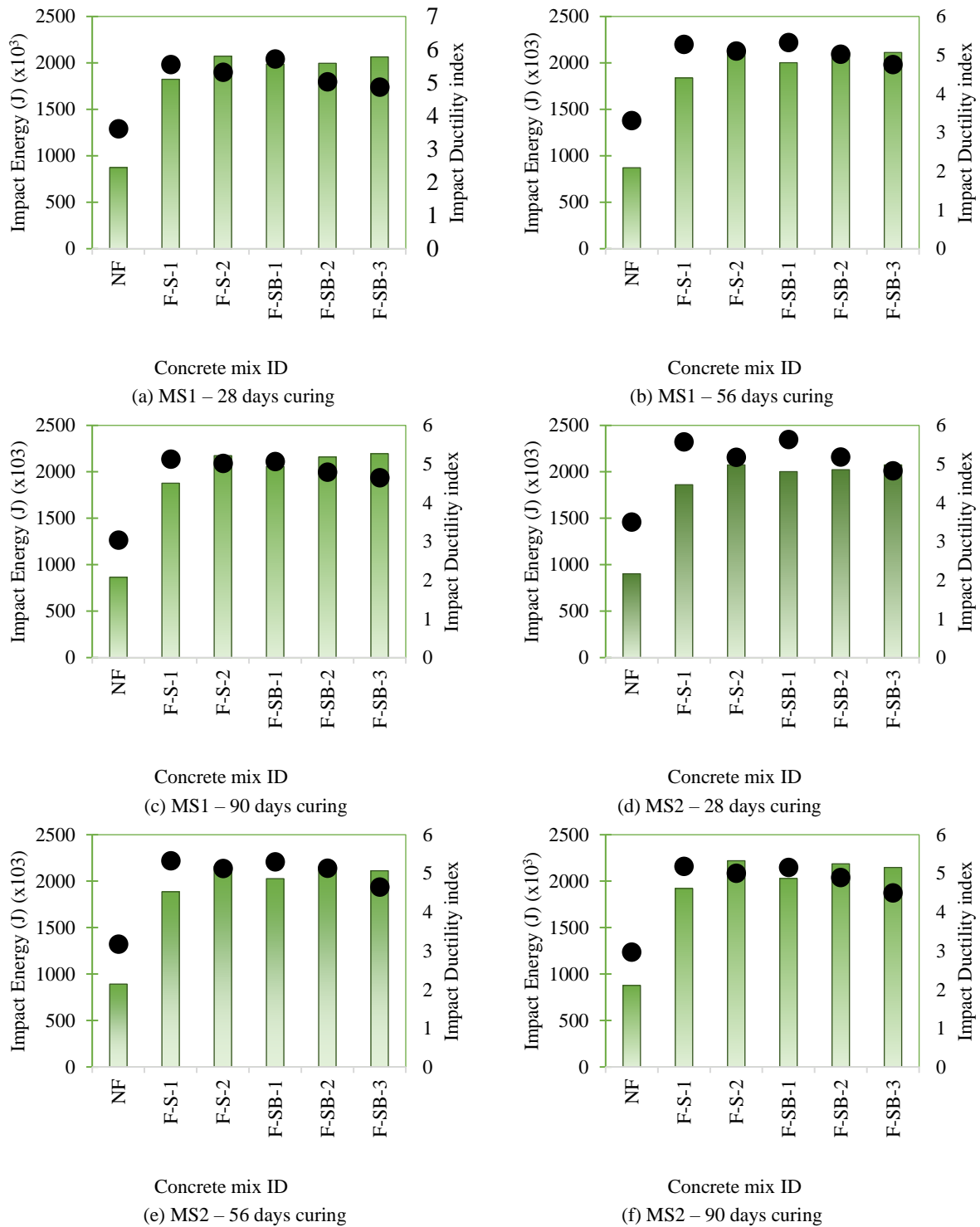


Figure 20. Post-cracking impact energy and ductility index.

In the case of impact energy, the crack initiation was early but still, the matrix endured an acceptable number of blows at which the specimen broke down into two pieces. The post-cracking energy reduces with the increased curing period ensuring the mix becomes denser with progressing hydration. NF using MS1 shows an average ductility index of 3.32, and using MS2, it was 3.22. These values expose that MS2 has no notable impact on the mechanical property than MS1. The NF performed

reasonably well, and it could grant better mechanical strengths but could not award appreciable failure patterns. It was evident that the omission of fibers affected not only the tensile property but also the counterbalance to meager deformations. Such defects forced the combination of fibers into the UHPC mix. Anas et al. (2022) also made identical conclusions that fibers are essential in building up certain mechanical and durability properties. The energy absorbed by the specimen with impact loading is determined by the number of blows, which are specified in Table 4.

The impact energy of F-S1 and F-S2 outperformed NF demonstrating an immense tolerance in the crack initiation. Moreover, the specimens with steel endured more blows after the first crack exposing an average of 60.53% and 67.11% boosted ductility indices with MS1 and MS2, respectively. With a further increased steel content, F-S-2 delivered a 55.54% and 59.19% increase in ductility than NF, with MS1 and MS2. Irrespective of MS1 and MS2, steel fibers are adroit in developing tensile strength and responsible for the solidarity of the structure. However, steel fibers are dense, which adds dead weight to the structure, and it eventually poses a corrosion threat as well. Their entire aversion is also a way out. The review on using natural fibers by Abdalla et al. (2023) also advises substituting natural fibers for better sustainability.

The decrease in ductility with increased fiber dosages might be due to the increase in density of the mixture, which aids in efficient packing. Figure 19 (a) to (f) specifies the energy sustained by the specimen till cracking and the final overall energy the specimen withstood. The resistance to impact by the specimens gradually increased when fiber dosage was increased. The F-SB-3 and F-S-2 mixture displayed similar resistance to impact, assuring that 3% of basalt can be substituted for 1% of steel when equivalent strength is needed. Figure 20 (a) to (f) shows that the lower fiber dosages also offered better post-cracking resistance with a slight average decrease of 4.10% and 3.70% by F-SB-1 and F-SB-2, respectively. The falloff in ductility indices with higher dosages in Figure 20 (a) to (f) might have resulted from the compact fiber-concrete bond, which delays the crack initiation. Tahwia et al., (2023) also conducted identical impact loading research on basalt fiber-reinforced high-performance concrete and expressed that basalt fiber promoted impact resistance.

The review of Al-Kharabsheh et al. (2023) guarantees that basalt fibers enrich the pore size distribution and ductility parameters. As far as the present study is concerned, no abrupt reduction in the mechanical properties was encountered with increasing fiber dosages. But the optimum dosage of fiber is limited to 3%, beyond which the flow significantly reduces, like the discussion by Wu et al. (2023) arrest the flow, and the mix does not satisfy the UHPC requirement. Basalt fibers also aid in durability, including reduced permeability, frost and temperature resistance, and protection from corrosion (Li et al., 2023).

4.4. Microstructure analysis

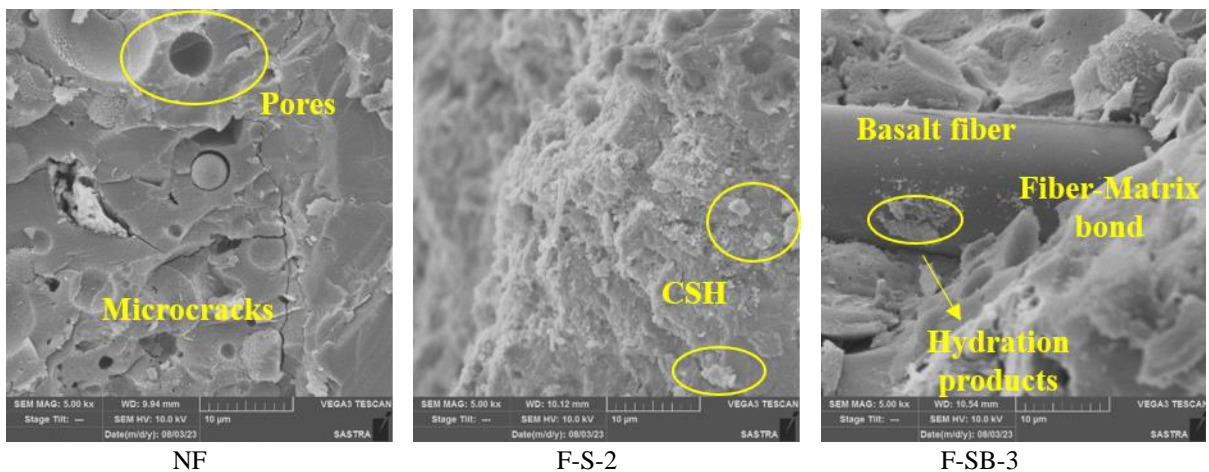


Figure 21. SEM images of UHPC.

To understand the matrices in a better way and validate the mechanical strength of fibrous concrete and several uncertainties in non-fibrous concrete, SEM imaging was conducted and is shown in Figure 21. It is evident that the presence of micro cracks and voids in the SEM of NF are reduced effectively when fibers are included. It can be clearly seen in Figure 21 (b) that the fiber incorporation formed an indiscrete matrix with dense microstructure. Steel fibers blocked crack development and significantly improved the resistance of the matrix against cracking. Similar observations by Zhang et al. (2022) reveal

that 12mm fibers are great candidates for resisting the propagation of cracks and deformation of the structure. They also scale down the crack area as an aftereffect of reducing the number and width of the cracks. The rapid strength progress in the matrices is due to the higher percentage existence of tricalcium silicate in OPC. There are considerable traces of CSH crystals, which, in combination with the fibers, are the reason for the mechanical performance. The random dispersion of fibers protected the matrix in all dimensions from cracking. The Sem observations of basalt fiber reinforced matrices sounded unscathed post-failure. F-SB-3 seemed almost identical to the microstructure study of basalt fibers by Chen et al. (2021), which carried mortar quantity barely expected to wrap the fiber, which is why further extension in fiber quantity resulted in balling effect.

4.5. Thermogravimetric analysis (TGA)

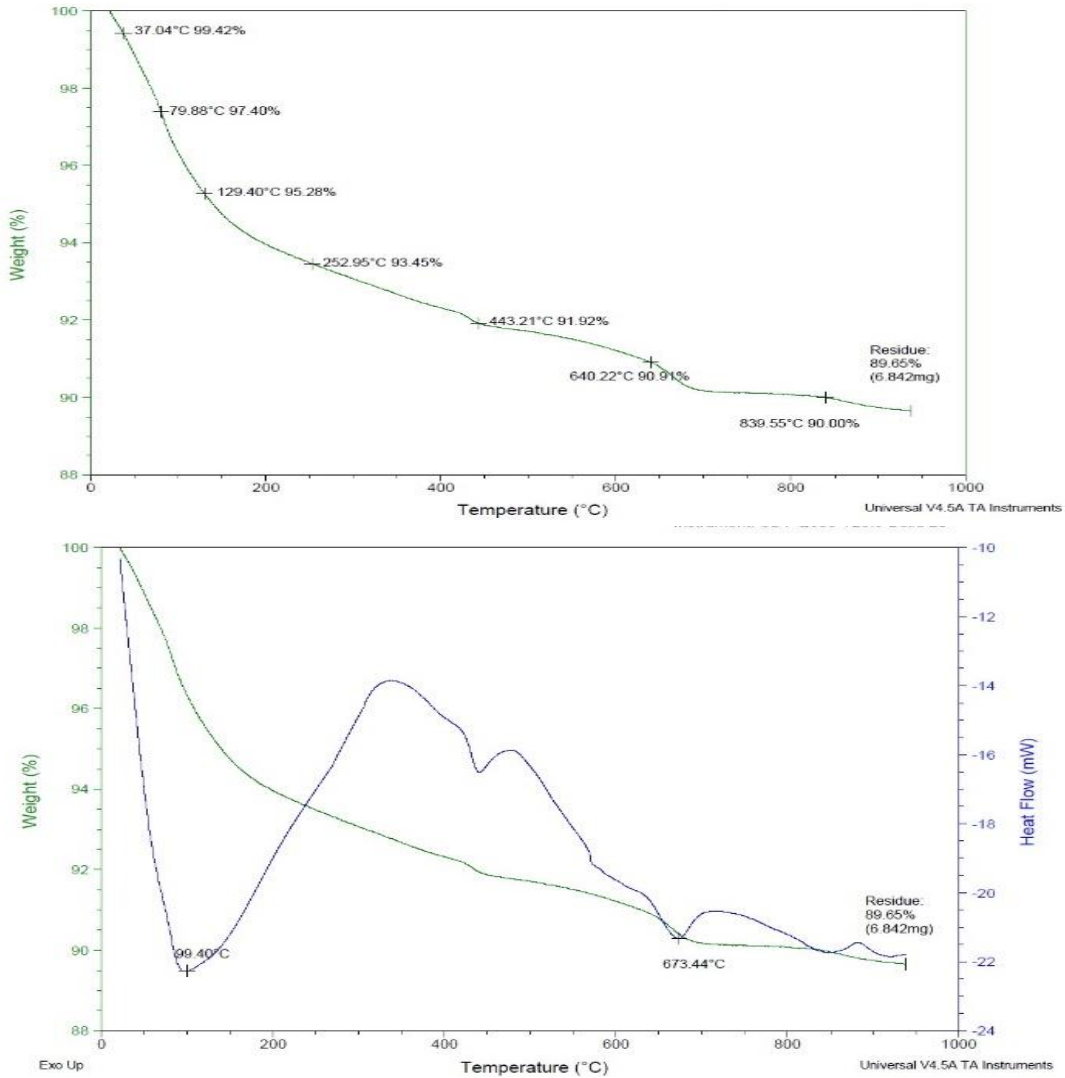


Figure 22. Thermogravimetry of F-S2.

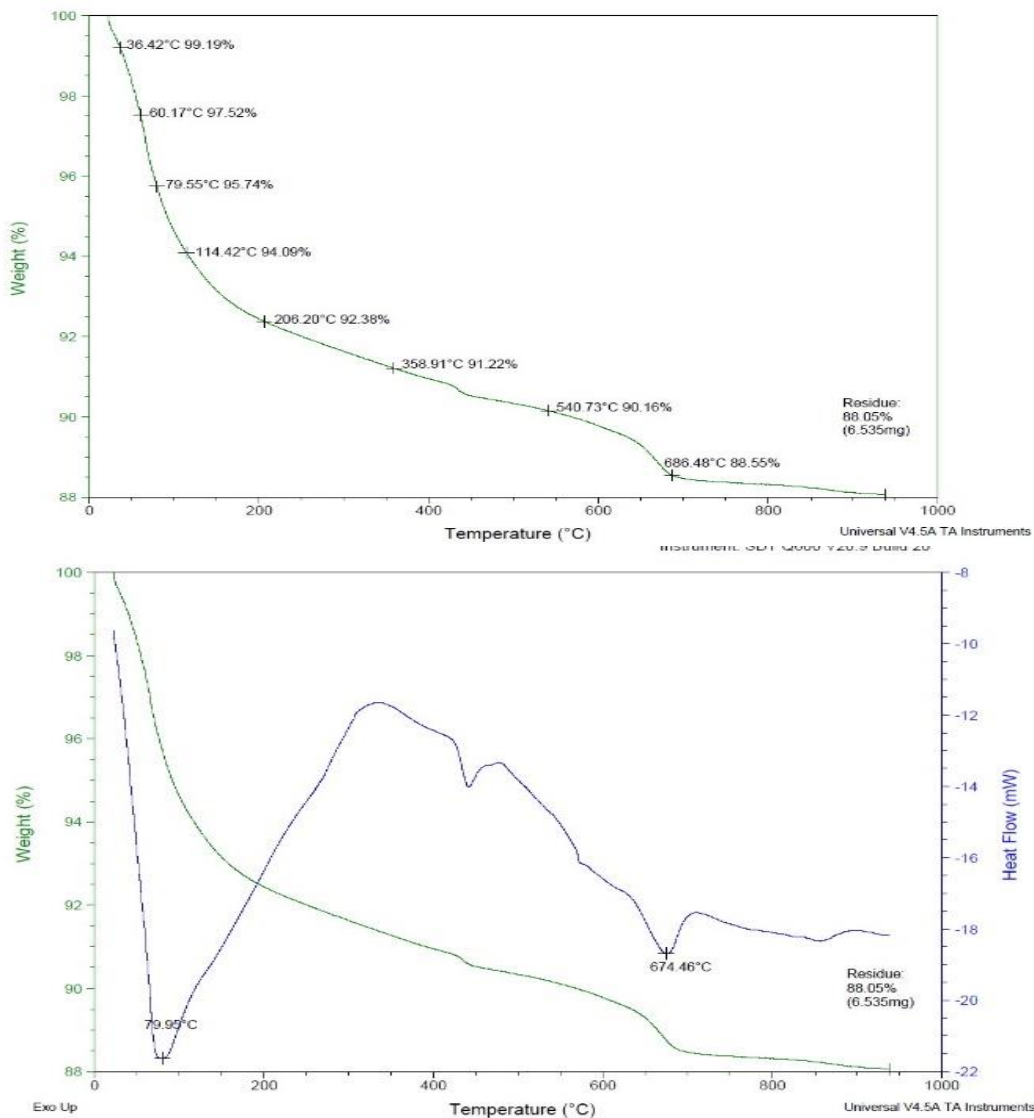


Figure 23. Thermogravimetry of F-SB3.

The 28-day cured samples of F-S-2 and F-SB-3 were thermogravimetrically analyzed the results are given in Figure 22 and 23. The mass loss curve in both images represents the decomposition of CSH crystals within a temperature range of 100-200°C. The primary element of the hydration products is ettringite, which also decomposes at similar temperature ranges. However, CSH was predominant, and no traces of ettringite were visualized in SEM imaging. The nano silicious particles in the mixture accelerated the cement hydration.

The mass loss between 400°C and 500°C temperature is probably attributable to the decomposition of CH constituents. The decreased presence of CH crystals might be due to the involvement of nanoparticles, as pronounced by Mostafa et al. (2020). The binding characteristic of concrete depends on CSH gel, where CH is only a secondary constituent and has very little contribution to the strength. The pozzolanic reactions between CH and nano-reactive components in the concrete form more CSH, which accounts for further mass loss on decomposition. The mass loss of UHPC contained hybrid basalt-steel fibers, and only steel fibers were almost equivalent; hence, it is advisable to substitute basalt fibers for steel fibers partly.

5. Conclusion

The study investigated the various basalt fiber dosages to partially take the place of steel fibers and received hopeful outcomes.

1. The MS1 mix, with 30% M-Sand, showed better compressive strength and impact resistance for different fiber dosages due to the optimum usage of the industrial waste M-sand and appropriate proportions of the fiber dosages.
2. In the compressive strength, MS1 mix with 1% steel fiber and 3% basalt fiber contributed to better compressive strength, and a maximum of 23.03% increase in strength was noticed. Though MS2 mix did not yield maximum strength, it possessed a compressive strength less by only 5.03% than the MS1 mix. The less workability due to the incorporation of more fibers and the use of more M-sand, overall, affected the strength characteristics of the MS2 mix.
3. The aforementioned fiber dosages performed better in resisting impact loading with MS1 resulting in worthy ductility indices.
4. The highest increment of 37.09% in splitting tensile strength was recorded for the same fiber combination but with 40% of manufactured sand.
5. The densely packed matrix was confirmed with the microstructure profiles of SEM, and the role of reactive components in the enrichment of the mechanical properties was validated using TGA.
6. The optimum basalt fiber dosage was determined to be 3%, over which the mixture becomes more fibrous in which the mortar was insufficient to wrap the fibers up into the shape.

Author contributions: P. Sujitha Magdalene: Conceptualization, Methodology, Visualization, Formal analysis, Writing – original draft.

B. Karthikeyan: Conceptualization, Methodology, Formal analysis, Writing – review & editing, Supervision, Project administration, Resources.

Funding: This project was carried out using the fund allotted to the TRR start-up research fund by SASTRA, which is Deemed to be a university.

Acknowledgments: The authors would like to acknowledge the financial support received from SASTRA Deemed to be University, Thanjavur, Tamil Nadu, India, for sanctioning required facilities through the TRR research grant. Ms. P. Sujitha Magdalene would like to acknowledge and is thankful to UGC for awarding the SJSJC fellowship (202223-UGCES-22-OB-TAM-F-SJSJC-9364).

Conflicts of interest: Authors declare that they have no conflict of interest to declare.

References

- Abbas, S., Nehdi, M. L., & Saleem, M. A. (2016). Ultra-High Performance Concrete: Mechanical Performance, Durability, Sustainability and Implementation Challenges. *International Journal of Concrete Structures and Materials*, 10(3), 271–295. <https://doi.org/10.1007/s40069-016-0157-4>
- Abdalla, J. A., Hawileh, R. A., Bahurudeen, A., Jyothsna, G., Sofi, A., Shanmugam, V., & Thomas, B. S. (2023). A comprehensive review on the use of natural fibers in cement/geopolymer concrete: A step towards sustainability. *Case Studies in Construction Materials*, 19, e02244. <https://doi.org/10.1016/j.cscm.2023.e02244>
- Abdulkareem, O. M., Ben Fraj, A., Bouasker, M., & Khelidj, A. (2018). Mixture design and early age investigations of more sustainable UHPC. *Construction and Building Materials*, 163, 235–246. <https://doi.org/10.1016/j.conbuildmat.2017.12.107>
- ACI 544 – 2R– 89. (2002). Measurement of Properties of Fiber Reinforced Concrete (Reapproved 2009).
- Aksoylu, C., Özkılıç, Y. O., Bahrami, A., Yıldız, S. A., Hakeem, I. Y., Özdöner, N., ... Karalar, M. (2023). Application of waste ceramic powder as a cement replacement in reinforced concrete beams toward sustainable usage in construction. *Case Studies in Construction Materials*, 19, e02444. <https://doi.org/10.1016/j.cscm.2023.e02444>
- Al-Kharabsheh, B. N., Arbili, M. M., Majdi, A., Alogla, S. M., Hakamy, A., Ahmad, J., & Deifalla, A. F. (2023). Basalt Fiber Reinforced Concrete: A Compressive Review on Durability Aspects. *Materials*, 16(1), 429. <https://doi.org/10.3390/ma16010429>

- Al-Rousan, E. T., Khalid, H. R., & Rahman, M. K. (2023). Fresh, mechanical, and durability properties of basalt fiber-reinforced concrete (BFRC): A review. *Developments in the Built Environment, 14*, 100155. <https://doi.org/10.1016/j.dibe.2023.100155>
- Anas, M., Khan, M., Bilal, H., Jadoon, S., & Khan, M. N. (2022). Fiber Reinforced Concrete: A Review. *ICEC 2022*, 3. Basel Switzerland: MDPI. <https://doi.org/10.3390/engproc2022022003>
- ASTM C150/C150M. (2022). Standard Specification for Portland Cement 1. https://doi.org/10.1520/C0150_C0150M-22
- ASTM C192/C192M. (2020). Standard Practice for Making and Curing Concrete Test Specimens in the Laboratory 1. https://doi.org/10.1520/C0192_C0192M-19
- ASTM C470/C470M. (2023). Standard Specification for Molds for Forming Concrete Test Cylinders Vertically 1. https://doi.org/10.1520/C0470_C0470M-23
- ASTM C1437. (2020). Standard Test Method for Flow of Hydraulic Cement Mortar 1. <https://doi.org/10.1520/C1437>
- ASTM C1856/C1856M. (2017). Standard Practice for Fabricating and Testing Specimens of Ultra-High Performance Concrete 1. https://doi.org/10.1520/C1856_C1856M-17
- ASTM D1557. (2021). Standard Test Methods for Laboratory Compaction Characteristics of Soil Using Modified Effort (56,000 ft-lbf/ft³ (2,700 kN-m/m³)) 1. <https://doi.org/10.1520/D1557-12R21>
- Bajaber, M. A., & Hakeem, I. Y. (2021). UHPC evolution, development, and utilization in construction: a review. *Journal of Materials Research and Technology, 10*, 1058–1074. <https://doi.org/10.1016/j.jmrt.2020.12.051>
- Chen, F., Xu, B., Jiao, H., Chen, X., Shi, Y., Wang, J., & Li, Z. (2021). Triaxial mechanical properties and microstructure visualization of BFRC. *Construction and Building Materials, 278*, 122275. <https://doi.org/10.1016/j.conbuildmat.2021.122275>
- Chu, H., Wang, F., Wang, L., Feng, T., & Wang, D. (2020). Mechanical Properties and Environmental Evaluation of Ultra-High-Performance Concrete with Aeolian Sand. *Materials, 13*(14), 3148. <https://doi.org/10.3390/ma13143148>
- de Klerk, M. D., Kayondo, M., Moelich, G. M., de Villiers, W. I., Combrinck, R., & Boshoff, W. P. (2020). Durability of chemically modified sisal fibre in cement-based composites. *Construction and Building Materials, 241*, 117835. <https://doi.org/10.1016/j.conbuildmat.2019.117835>
- Dingqiang, F., Yu, R., Kangning, L., Junhui, T., Zhonghe, S., Chunfeng, W., ... Qiqi, S. (2021). Optimized design of steel fibres reinforced ultra-high performance concrete (UHPC) composites: Towards to dense structure and efficient fibre application. *Construction and Building Materials, 273*, 121698. <https://doi.org/10.1016/j.conbuildmat.2020.121698>
- Du, J., Meng, W., Khayat, K. H., Bao, Y., Guo, P., Lyu, Z., ... Wang, H. (2021). New development of ultra-high-performance concrete (UHPC). *Composites Part B: Engineering, 224*, 109220. <https://doi.org/10.1016/j.compositesb.2021.109220>
- Gao, L., Adesina, A., & Das, S. (2021). Properties of eco-friendly basalt fibre reinforced concrete designed by Taguchi method. *Construction and Building Materials, 302*, 124161. <https://doi.org/10.1016/j.conbuildmat.2021.124161>
- Ghafari, E., Costa, H., & Júlio, E. (2015). Critical review on eco-efficient ultra high performance concrete enhanced with nano-materials. *Construction and Building Materials, 101*, 201–208. <https://doi.org/10.1016/j.conbuildmat.2015.10.066>
- Harish, B. A., Hanumesh, B. M., Venkata Ramana, N., & Gnaneswar, K. (2023). Assessment of mechanical properties of recycled coarse aggregate concrete incorporating basalt and polypropylene fiber. *Materials Today: Proceedings*. <https://doi.org/10.1016/j.matpr.2023.06.196>
- Hou, X., Cao, S., Rong, Q., Zheng, W., & Li, G. (2018). Effects of steel fiber and strain rate on the dynamic compressive stress-strain relationship in reactive powder concrete. *Construction and Building Materials, 170*, 570–581. <https://doi.org/10.1016/j.conbuildmat.2018.03.101>
- Huang, K., Xie, J., Feng, Y., Wang, R., & Ji, J. (2023). Axial impact behaviors of UHPC: The roles of nanomaterials and steel fibres. *Construction and Building Materials, 384*, 131396. <https://doi.org/10.1016/j.conbuildmat.2023.131396>
- IS-4031 (PART 6). (1988). *Methods of Physical Tests for Hydraulic Cement (Reaffirmed 2000)*.
- Jabbar, A. M., Hamood, M. J., & Mohammed, D. H. (2021). The effect of using basalt fibers compared to steel fibers on the shear behavior of ultra-high performance concrete T-beam. *Case Studies in Construction Materials, 15*, e00702. <https://doi.org/10.1016/j.cscm.2021.e00702>
- Janković, K., Stanković, S., Bojović, D., Stojanović, M., & Antić, L. (2016). The influence of nano-silica and barite aggregate on properties of ultra high performance concrete. *Construction and Building Materials, 126*, 147–156. <https://doi.org/10.1016/j.conbuildmat.2016.09.026>
- Karalar, M. (2020). Experimental and Numerical Investigation on Flexural and Crack Failure of Reinforced Concrete Beams with Bottom Ash and Fly Ash. *Iranian Journal of Science and Technology, Transactions of Civil Engineering, 44*(S1), 331–354. <https://doi.org/10.1007/s40996-020-00465-y>
- Karalar, M., Ozturk, H., & Ozkilic, Y. O. (2023). Experimental and numerical investigation on flexural response of reinforced rubberized concrete beams using waste tire rubber. *Steel and Composite Structures, 48*(1), 43–57.
- Khan, M., Lao, J., Ahmad, M. R., & Dai, J.-G. (2024). Influence of high temperatures on the mechanical and microstructural properties of hybrid steel-basalt fibers based ultra-high-performance concrete (UHPC). *Construction and Building Materials, 411*, 134387. <https://doi.org/10.1016/j.conbuildmat.2023.134387>

- Kim, D. J., Park, S. H., Ryu, G. S., & Koh, K. T. (2011). Comparative flexural behavior of Hybrid Ultra High Performance Fiber Reinforced Concrete with different macro fibers. *Construction and Building Materials*, 25(11), 4144–4155. <https://doi.org/10.1016/j.conbuildmat.2011.04.051>
- Korkut, F., & Karalar, M. (2023). Investigational and Numerical Examination on Bending Response of Reinforced Rubberized Concrete Beams Including Plastic Waste. *Materials*, 16(16), 5538. <https://doi.org/10.3390/ma16165538>
- Li, F., Lv, T., & Wei, S. (2023). Performance, Mechanical Properties and Durability of a New Type of UHPC—Basalt Fiber Reinforced Reactive Powder Concrete: A Review. *Polymers*, 15(14), 3129. <https://doi.org/10.3390/polym15143129>
- Li, Z., Shen, A., Zeng, G., Chen, Z., & Guo, Y. (2022). Research progress on properties of basalt fiber-reinforced cement concrete. *Materials Today Communications*, 33, 104824. <https://doi.org/10.1016/j.mtcomm.2022.104824>
- Liu, K., Song, R., Li, J., Guo, T., Li, X., Yang, J., & Yan, Z. (2022). Effect of steel fiber type and content on the dynamic tensile properties of ultra-high performance cementitious composites (UHPC). *Construction and Building Materials*, 342, 127908. <https://doi.org/10.1016/j.conbuildmat.2022.127908>
- Magdalene, P. S., Raj, P., Priya, G., Karthikeyan, B., Selvaraj, S. K., & Azab, M. (2023). Experimental study and statistical validation of UHSM made with industrial wastes and hybrid fibres. *International Journal on Interactive Design and Manufacturing (IJIDeM)*, 17(6), 3133–3148. <https://doi.org/10.1007/s12008-023-01382-v>
- Merin Philip, P., Joseph, A., Zachariah Koshy, R., & Jossy, A. (2023). Mechanical and permeability properties of basalt fibre Reinforced concrete. *Materials Today: Proceedings*. <https://doi.org/10.1016/j.matpr.2023.05.133>
- Mohammed, B. H., Sherwani, A. F. H., Faraj, R. H., Qadir, H. H., & Younis, K. H. (2021). Mechanical properties and ductility behavior of ultra-high performance fiber reinforced concretes: Effect of low water-to-binder ratios and micro glass fibers. *Ain Shams Engineering Journal*, 12(2), 1557–1567. <https://doi.org/10.1016/j.asej.2020.11.008>
- Mostafa, S. A., Fariad, A. S., Farghali, A. A., EL-Deeb, M. M., Tawfik, T. A., Majer, S., & Abd Elrahman, M. (2020). Influence of Nanoparticles from Waste Materials on Mechanical Properties, Durability and Microstructure of UHPC. *Materials*, 13(20), 4530. <https://doi.org/10.3390/ma13204530>
- Onur Pehlivan, A. (2022). Effect of silica fume and basalt fibers on the fracture parameters of magnesium phosphate cement incorporating fly ash. *Revista de La Construcción*, 21(3), 523–538. <https://doi.org/10.7764/RDLC.21.3.523>
- Park, S. H., Kim, D. J., Ryu, G. S., & Koh, K. T. (2012). Tensile behavior of Ultra High Performance Hybrid Fiber Reinforced Concrete. *Cement and Concrete Composites*, 34(2), 172–184. <https://doi.org/10.1016/j.cemconcomp.2011.09.009>
- Prasad, V. D., Prakash, E. L., Abishek, M., Ushanth Dev, K., & Sanjay Kiran, C. K. (2018). Study on concrete containing Waste Foundry Sand, Fly Ash and Polypropylene fibre using Taguchi Method. *Materials Today: Proceedings*, 5(11), 23964–23973. <https://doi.org/10.1016/j.matpr.2018.10.189>
- Qi, J., Wu, Z., Ma, Z. J., & Wang, J. (2018). Pullout behavior of straight and hooked-end steel fibers in UHPC matrix with various embedded angles. *Construction and Building Materials*, 191, 764–774. <https://doi.org/10.1016/j.conbuildmat.2018.10.067>
- Ren, G., Yao, B., Huang, H., & Gao, X. (2021). Influence of sisal fibers on the mechanical performance of ultra-high performance concretes. *Construction and Building Materials*, 286, 122958. <https://doi.org/10.1016/j.conbuildmat.2021.122958>
- Rui, Y., Kangning, L., Tianyi, Y., Liwen, T., Mengxi, D., & Zhonghe, S. (2022). Comparative study on the effect of steel and polyoxymethylene fibers on the characteristics of Ultra-High Performance Concrete (UHPC). *Cement and Concrete Composites*, 127, 104418. <https://doi.org/10.1016/j.cemconcomp.2022.104418>
- Sharma, R., Jang, J. G., & Bansal, P. P. (2022). A comprehensive review on effects of mineral admixtures and fibers on engineering properties of ultra-high-performance concrete. *Journal of Building Engineering*, 45, 103314. <https://doi.org/10.1016/j.jobbe.2021.103314>
- Sujitha Magdalene, P., Karthikeyan, B., Selvaraj, S. K., Deepika, S., Alqaryouti, Y., Seif ElDin, H. M., & Azab, M. (2023). Ultra-high-performance concrete with Iron ore tailings and non-metallic and hybrid fibers-A comprehensive experimental study. *Case Studies in Construction Materials*, 19, e02544. <https://doi.org/10.1016/j.cscm.2023.e02544>
- Tahwia, A. M., Helal, K. A., & Youssf, O. (2023). Chopped Basalt Fiber-Reinforced High-Performance Concrete: An Experimental and Analytical Study. *Journal of Composites Science*, 7(6), 250. <https://doi.org/10.3390/jcs7060250>
- Van Tuan, N., Ye, G., van Breugel, K., Fraaij, A. L. A., & Bui, D. D. (2011). The study of using rice husk ash to produce ultra high performance concrete. *Construction and Building Materials*, 25(4), 2030–2035. <https://doi.org/10.1016/j.conbuildmat.2010.11.046>
- Voit, K., & Kimbauer, J. (2014). Tensile characteristics and fracture energy of fiber reinforced and non-reinforced ultra high performance concrete (UHPC). *International Journal of Fracture*, 188(2), 147–157. <https://doi.org/10.1007/s10704-014-9951-7>
- Wang, D., Shi, C., Wu, Z., Xiao, J., Huang, Z., & Fang, Z. (2015). A review on ultra high performance concrete: Part II. Hydration, microstructure and properties. *Construction and Building Materials*, 96, 368–377. <https://doi.org/10.1016/j.conbuildmat.2015.08.095>
- Wang, X., Wu, D., Zhang, J., Yu, R., Hou, D., & Shui, Z. (2021). Design of sustainable ultra-high performance concrete: A review. *Construction and Building Materials*, 307, 124643. <https://doi.org/10.1016/j.conbuildmat.2021.124643>
- Wiemer, N., Wetzel, A., Schleiting, M., Krooß, P., Vollmer, M., Niendorf, T., ... Middendorf, B. (2020). Effect of Fibre Material and Fibre Roughness on the Pullout Behaviour of Metallic Micro Fibres Embedded in UHPC. *Materials*, 13(14), 3128. <https://doi.org/10.3390/ma13143128>

- Wu, H., Qin, X., Huang, X., & Kaewunruen, S. (2023). Engineering, Mechanical and Dynamic Properties of Basalt Fiber Reinforced Concrete. *Materials*, 16(2), 623. <https://doi.org/10.3390/ma16020623>
- Wu, Z., Shi, C., He, W., & Wang, D. (2016). Uniaxial Compression Behavior of Ultra-High Performance Concrete with Hybrid Steel Fiber. *Journal of Materials in Civil Engineering*, 28(12). [https://doi.org/10.1061/\(ASCE\)MT.1943-5533.0001684](https://doi.org/10.1061/(ASCE)MT.1943-5533.0001684)
- Wu, Z., Shi, C., Khayat, K. H., & Xie, L. (2018). Effect of SCM and nano-particles on static and dynamic mechanical properties of UHPC. *Construction and Building Materials*, 182, 118–125. <https://doi.org/10.1016/j.conbuildmat.2018.06.126>
- Yan, P., Chen, B., Afgan, S., Aminul Haque, M., Wu, M., & Han, J. (2021). Experimental research on ductility enhancement of ultra-high performance concrete incorporation with basalt fibre, polypropylene fibre and glass fibre. *Construction and Building Materials*, 279, 122489. <https://doi.org/10.1016/j.conbuildmat.2021.122489>
- Yang, J., Chen, B., Su, J., Xu, G., Zhang, D., & Zhou, J. (2022). Effects of fibers on the mechanical properties of UHPC: A review. *Journal of Traffic and Transportation Engineering (English Edition)*, 9(3), 363–387. <https://doi.org/10.1016/j.jtte.2022.05.001>
- Yang, R., Yu, R., Shui, Z., Gao, X., Xiao, X., Fan, D., ... He, Y. (2020). Feasibility analysis of treating recycled rock dust as an environmentally friendly alternative material in Ultra-High Performance Concrete (UHPC). *Journal of Cleaner Production*, 258, 120673. <https://doi.org/10.1016/j.jclepro.2020.120673>
- Yoo, D.-Y., Kim, S., Park, G.-J., Park, J.-J., & Kim, S.-W. (2017). Effects of fiber shape, aspect ratio, and volume fraction on flexural behavior of ultra-high-performance fiber-reinforced cement composites. *Composite Structures*, 174, 375–388. <https://doi.org/10.1016/j.compstruct.2017.04.069>
- Yoo, D.-Y., & Yoon, Y.-S. (2015). Structural performance of ultra-high-performance concrete beams with different steel fibers. *Engineering Structures*, 102, 409–423. <https://doi.org/10.1016/j.engstruct.2015.08.029>
- Yu, R., Spiesz, P., & Brouwers, H. J. H. (2015). Development of an eco-friendly Ultra-High Performance Concrete (UHPC) with efficient cement and mineral admixtures uses. *Cement and Concrete Composites*, 55, 383–394. <https://doi.org/10.1016/j.cemconcomp.2014.09.024>
- Zhang, A., Liu, K., Li, J., Song, R., & Guo, T. (2024). Static and dynamic tensile properties of ultra-high performance concrete (UHPC) reinforced with hybrid sisal fibers. *Construction and Building Materials*, 411, 134492. <https://doi.org/10.1016/j.conbuildmat.2023.134492>
- Zhang, G.-Z., & Wang, X.-Y. (2020). Effect of Pre-Wetted Zeolite Sands on the Autogenous Shrinkage and Strength of Ultra-High-Performance Concrete. *Materials*, 13(10), 2356. <https://doi.org/10.3390/ma13102356>
- Zhang, H., Ji, T., & Lin, X. (2019). Pullout behavior of steel fibers with different shapes from ultra-high performance concrete (UHPC) prepared with granite powder under different curing conditions. *Construction and Building Materials*, 211, 688–702. <https://doi.org/10.1016/j.conbuildmat.2019.03.274>
- Zhang, J., Zhao, Y., & Li, H. (2017). Experimental Investigation and Prediction of Compressive Strength of Ultra-High Performance Concrete Containing Supplementary Cementitious Materials. *Advances in Materials Science and Engineering*, 2017, 1–8. <https://doi.org/10.1155/2017/4563164>
- Zhang, W., Zheng, M., Zhu, L., Ren, Y., & Lv, Y. (2022). Investigation of steel fiber reinforced high-performance concrete with full aeolian sand: Mix design, characteristics and microstructure. *Construction and Building Materials*, 342, 128065. <https://doi.org/10.1016/j.conbuildmat.2022.128065>
- Zhang, W., Zou, X., Wei, F., Wang, H., Zhang, G., Huang, Y., & Zhang, Y. (2019). Grafting SiO₂ nanoparticles on polyvinyl alcohol fibers to enhance the interfacial bonding strength with cement. *Composites Part B: Engineering*, 162, 500–507. <https://doi.org/10.1016/j.compositesb.2019.01.034>
- Zhang, Y., Zhu, Y., Qiu, J., Hou, C., & Huang, J. (2023). Impact of reinforcing ratio and fiber volume on flexural hardening behavior of steel reinforced UHPC beams. *Engineering Structures*, 285, 116067. <https://doi.org/10.1016/j.engstruct.2023.116067>
- Zhou, H., Zhu, H., Gou, H., & Yang, Z. (2020). Comparison of the Hydration Characteristics of Ultra-High-Performance and Normal Cementitious Materials. *Materials*, 13(11), 2594. <https://doi.org/10.3390/ma13112594>



Copyright (c) 2024 Magdalene, P., Karthikeyan, B. This work is licensed under a [Creative Commons Attribution-Noncommercial-No Derivatives 4.0 International License](https://creativecommons.org/licenses/by-nc-nd/4.0/).